



<http://sciforum.net/conference/ece-1>

Conference Proceedings Paper - Energies „Whither Energy Conversion? Present Trends, Current Problems and Realistic Future Solutions”

Hydrogen Storage in Boron Nitride and Carbon Nanomaterials

Takeo Oku*

Department of Materials Science, The University of Shiga Prefecture, Hassaka 2500, Hikone, Shiga 522-8533, Japan; E-Mail: oku@mat.usp.ac.jp

* Author to whom correspondence should be addressed; E-Mail: oku@mat.usp.ac.jp (T.O.); Tel.: +81-749-28-8368; Fax: +81-749-28-8590.

Received: 16 January 2014 / Accepted: 18 March 2014 / Published: 18 March 2014

Abstract: Boron nitride (BN) nanomaterials were synthesized from LaB₆ and Pd/boron powder, and the hydrogen storage was investigated by differential thermogravimetric analysis, which showed possibility of hydrogen storage of 1–3 wt%. The hydrogen gas storage in BN and carbon (C) clusters was also investigated by molecular orbital calculations, which indicated possible hydrogen storage of 6.5 and 4.9 wt%, respectively. Chemisorption calculation was also carried out for B₂₄N₂₄ cluster with changing endohedral elements in BN cluster to compare the bonding energy at nitrogen and boron, which showed that Li is a suitable element for hydrogenation to the BN cluster. The BN cluster materials would store H₂ molecule easier than carbon fullerene materials, and its stability for high temperature would be good. Molecular dynamics calculations showed that a H₂ molecule remains stable in a C₆₀ cage at 298 K and 0.1 MPa, and that pressures over 5 MPa are needed to store H₂ molecules in the C₆₀ cage.

Keywords: nanostructure; boron nitride; carbon; hydrogen gas storage; hydrogenation; molecular orbital calculation

1. Introduction

Hydrogen is a carrier with high energy density, and forms only water and heat. On the other hand, fossil fuels generate toxic fuels such as CO_x, NO_x and SO_x. Therefore, clean hydrogen energy is expected as substitute of fossil fuel in 21st century, and gas storage ability more than 6.5 wt% is needed for car application according to the US Department of Energy. Although LaNi₅H₆ is already

used as H₂ gas storage materials, the ability is only 1 wt% because of large atomic number of La and Ni [1]. On the other hand, fullerene-like materials, which consist of light elements such as boron, carbon and nitrogen, would store more H₂ gas compared to the metal hydrides. Various works have been reported on hydrogen storage ability of carbon nanotubes, fullerenes and nanomaterials [1]. It was reported that multi-walled carbon nanotubes could absorb hydrogen from 1 wt% up to 4.6 wt%. These results indicate carbon nanotubes might be a possible candidate of hydrogen storage materials although the evaluation of hydrogen storage measurements is necessary. Recently, several studies on H₂ gas storage in boron nitride (BN) nanomaterials have been reported [2–7]. BN nanomaterials are expected in prospective application because they provide good stability at high temperatures with high electronic insulation in air [8]. It is difficult to absorb hydrogen by physisorption both inside nanotubes and at the interstitial channels of nanotubes at room temperature, which is due to too weak bonding of physisorbed hydrogen to reach large storage at room temperature. Therefore, it is considered that chemisorption is a necessary requirement for hydrogen storage at room temperature. It was reported that chemisorption ratio observed at room temperature increases with increasing alkali/carbon rate. Therefore, if the energy of chemisorption can be lowered, hydrogen storage ability of carbon and BN nanotubes would be improved.

The purpose of the present study is twofold. The first is to prepare BN nanotubes, nanocapsules and nanocages, and to investigate hydrogen gas storage by thermogravimetry/differential thermogravimetric analysis (TG/DTA) and first principle calculation. LaB₆ and Pd were selected in order to take advantage of their catalytic effect to produce the BN nanomaterials. La has shown excellent catalytic properties for producing a large number of single-walled carbon nanotubes and enlarging their diameter, and Pd is also expected to act as a hydrogen storage material. Although gas storage of hydrogen and argon in carbon nanotubes has been reported, carbon nanotubes are oxidized at 600 °C in air. On the other hand, BN are stable up to 1000 °C in air [8], which indicates the excellent heat resistance compared to the carbon materials for gas storage. To understand the formation of BN nanostructures, high-resolution electron microscopy (HREM) were carried out, which are very powerful methods for atomic structure analysis [9]. For the BN nanomaterials, hydrogen gas storage measurements were carried out using TG/DTA.

The second purpose of the present work is to investigate H₂ gas storage ability of BN and C fullerene-like materials by theoretical calculation. Although huge amount of calculation is required to calculate nanotubes, it is considered that H₂ molecules enter from the cap of nanotubes. Energy of chemisorption and stable hydrogen position inside the clusters were investigated as cap structures of nanotubes. Influence of endohedral element on H₂ gas storage ability of BN fullerene-like materials was also investigated by theoretical calculations. Energy of chemisorption was investigated for cage clusters as a cap structure of nanotubes, and B₂₄N₂₄ clusters, reported by mass spectrometry [8], were selected for the storage material. Li, K and Na elements were also selected for the doping atoms because these elements are of high electropositive character. The present study will give us a guideline for hydrogenation of BN nanomaterials as hydrogen storage materials.

2. Hydrogen storage in BN nanomaterials studied by TG/DTA

Mixture powder compacts made of boron particles (99%, 40 μm , Niraco Co. Ltd), LaB_6 particles (99%, 1 μm , Wako) and Pd particles (99.5%, 0.1 μm , Niraco), with the size of 3 mm in height and 30 mm in diameter were produced by pressing powder at 10 MPa. The atomic ratios of metal (M) to boron (B) were in the range of 1:1–1:10. The green compacts were set on a copper mold in an electric-arc furnace, which was evacuated down to 2.0×10^{-3} Pa. After introducing a mixed gas of Ar 0.025 MPa and N_2 0.025 MPa, arc-melting was applied to the samples at an accelerating voltage of 200 V and an arc current of 125 A for 2 s. Arc-melting was performed with a vacuum arc-melting furnace (NEV-AD03, Nisshin Engineering), and the white/gray BN nanomaterial powders were collected from surface of the bulk. Samples for HREM observation were prepared by dispersing the materials on holey carbon grids. HREM observation was performed with a 300 kV electron microscope (JEM-3000F). To confirm the formation of BN fullerene materials, energy dispersive x-ray spectroscopy analysis was performed using the EDAX system with a probe size of ~ 10 nm. In order to measure hydrogen gas storage in BN nanomaterials, BN nanomaterials were extracted from the obtained powder by a supersonic dispersing method based on the Stokes equation using ethanol. The Stokes equation is expressed as follows: $v = d^2(\sigma - \rho)g/18\eta$ ($h = vt$; v ; sedimentation rate, η ; viscosity of liquid, σ ; density of particles, ρ ; density of liquid, g ; gravitational acceleration, d ; diameter of particles, t ; subsidence time, h ; height of liquid). Since there is a big difference in the size and density of the produced BN nanocapsules/nanotubes and other powders, it is believed that this method would be effective for separation of BN nanomaterials. After separation of BN nanomaterials, hydrogen storage was measured by TG/DTA at temperatures in the range of 20–300 $^\circ\text{C}$ in H_2 atmosphere [10].

Figure 1. HREM images of BN nanotube and BN nanocapsules produced using powder with ratios of (a) La:B = 1:6, (b) La:B = 1:4, and (c) Pd:B = 1:4.

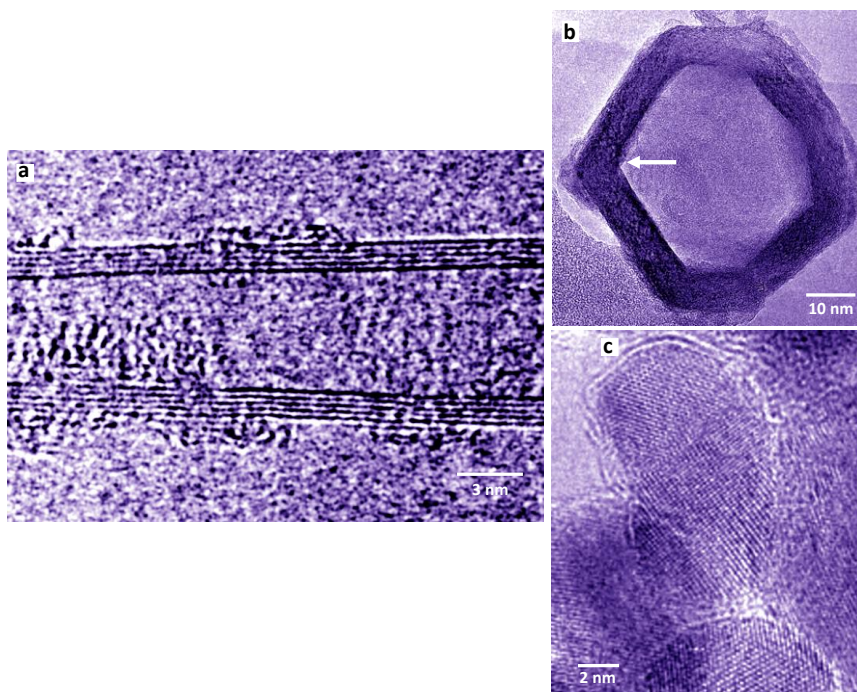


Figure 2. DTA and TG curve of BN nanocapsules and nanotubes produced using LaB_6 powder.

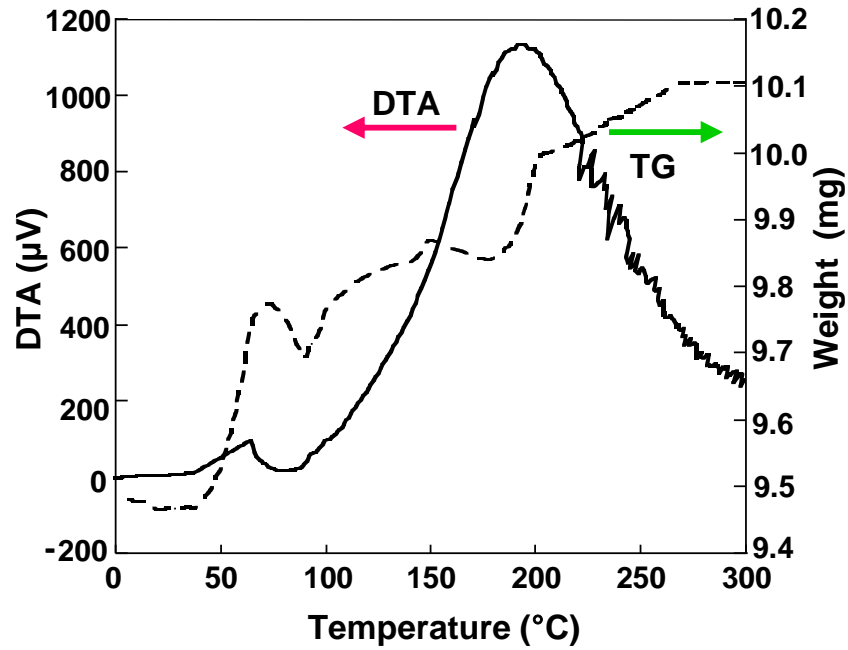


Figure 3. Structure models that H_2 molecule passes through hexagonal BN rings of (a), (b) tip of $\text{B}_{99}\text{N}_{99}$ nanotube and (c) $\text{B}_{36}\text{N}_{36}$ cluster.

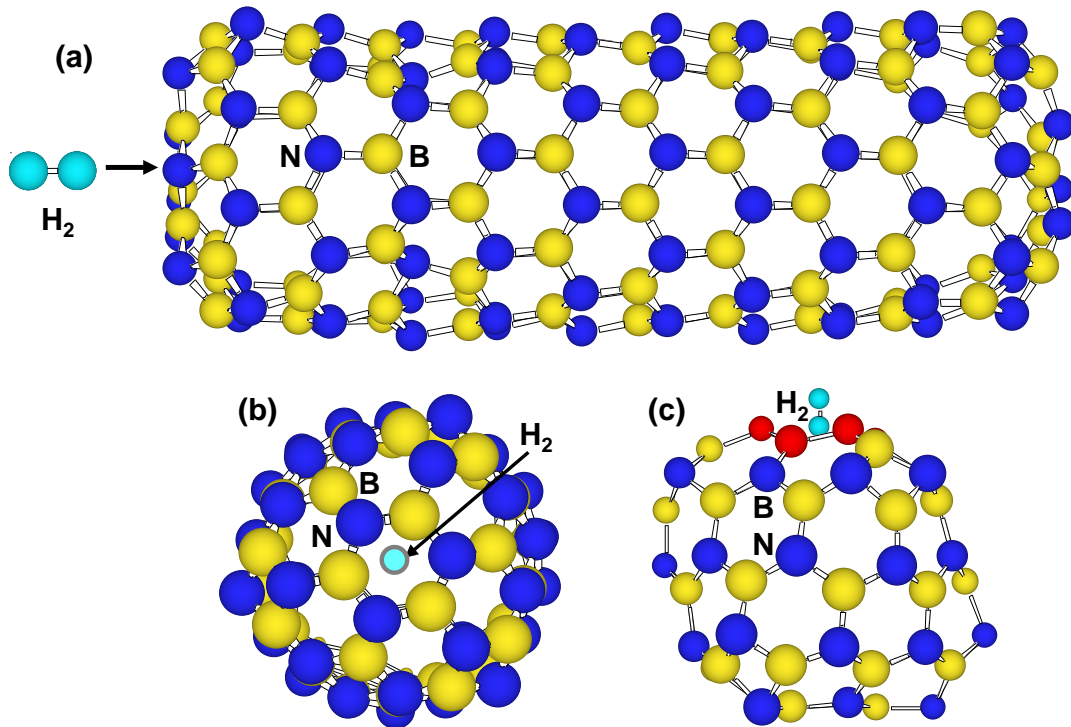


Table 1. Atomic ratio of starting materials, produced structures and hydrogen storage.

M:B	Nanostructures	Weight change (wt%)
La:B = 1:6	Nanotubes and nanocages	+3.2
La:B = 1:10	Nanotubes	+0.58
Pd:B = 1:4	Nanocapsules	+1.6

To search the optimized structure of $B_{99}N_{99}$ and $B_{36}N_{36}$ with H_2 molecules, semi-empirical molecular orbital calculations (PM3) were performed. The energies of $B_{36}N_{36}$ with H_2 molecules were calculated by first principle single point energy calculation using Gaussian. In the calculation, 3-21G was used as ground function with Hartree–Fock level.

A HREM image of a BN nanotube produced using LaB_6 powder is shown in Figure 1(a). In Figure 1(a), the diameter of the five-layered BN nanotube is changing from bottom to top, and amorphous patches are observed mostly at the top. A HREM image of BN nanocage produced from LaB_6/B powder is shown in Figure 1(b), which indicates square-like shape, and four-membered rings of BN exist at the corner of the cage. The BN nanocage has a network-like structure, whose atomic arrangement is basically consistent with the $B_{36}N_{36}$ cluster structure [9]. BN nanocapsules with Pd nanoparticles were also produced as shown in Figure 1(c), and Pd nanoparticles were covered by a few BN layers. In order to confirm the formation of BN nanocapsules, EDX analysis was carried out, which showed the atomic ratio of B:N ~1.

DTA and TG curve of BN nanomaterials produced from LaB_6 powder is shown in Figure 2. At a temperature around 70 °C, an increase of sample weight of 0.3 mg is observed. Weight change for this sample was almost reversible, which indicates the reversibility of hydrogen adsorption. It also suggests that the hydrogen atoms would be physically absorbed. For the samples of La:B = 1:6 and Pd:B = 1:4, weight increases of 3.2 and 1.6% were observed, respectively, as listed in Table 1.

BN nanostructures would have energy barriers for H_2 molecules to pass through tetragonal and hexagonal rings. Figure 3 are structure models in which H_2 molecule passes from hexagonal rings of $B_{99}N_{99}$ and $B_{36}N_{36}$. Single point energies were calculated with changing set point of H_2 molecule from the center of the cage at intervals of 0.1 nm. There is energy barrier that is given for H_2 molecules to pass through the hexagonal rings. The energy barrier of $B_{36}N_{36}$ hexagonal rings showed the smallest value of 14 eV in the present calculation, which is smaller than that of 27 eV at tetragonal rings. The DE of C_{60} hexagonal rings was also calculated to be 16 eV for comparison. This value is higher than that of $B_{36}N_{36}$ hexagonal rings, and the H_2 molecule would pass from hexagonal rings of $B_{36}N_{36}$ easier than from hexagonal rings of C_{60} . It is known that H_2 molecules are adsorbed on walls of single-walled carbon nanotubes over 7 MPa as an experimental result. As a result of the comparison, H_2 molecules enter into $B_{36}N_{36}$ from hexagonal rings easier than tetragonal rings $B_{36}N_{36}$ and hexagonal rings of C_{60} .

A formation mechanism of BN nanotubes and nanocapsules synthesized in the present work is described below. Metal and boron particles are melted by arc-melting, and during the solidification of the liquid into metal and/or boride nanoparticles, excess boron would react with nitrogen to form BN layers at the surface of the nanoparticles. Because of electrical insulation, BN fullerene materials are

usually fabricated by arc-discharge method with specific conducting electrodes such as HfB_2 and ZrB_2 . The present arc-melting method from mixed powder has two advantages for BN nanomaterial production. Since the powder becomes conducting by pressing, special electrodes are not needed. In addition, ordinary, commercial arc-melting furnaces can be used. These advantages indicate a simpler fabrication method compared to the ordinary arc-discharge methods.

Although gas storages of hydrogen and argon in carbon nanotubes have been reported, there are few reports for gas storage in BN fullerene materials and for calculations [10]. Weight increase of the sample in TG measurements was observed as shown in Figure 2. It might be due to the hydrogen gas storage in the BN nanomaterials. Since there would be metal and boron nanoparticles in the separated BN nanomaterials even after the separation, further qualification and evaluation of the samples are needed for hydrogen storage.

Carbon fullerenes and boron nitride fullerenes are sublimed at 600 and 1000 °C, respectively. Boron nitride fullerenes would storage H_2 molecules with smaller energy than carbon fullerenes, and would give good stability at high temperature. Boron nitride fullerene materials would be better candidate for H_2 storage materials.

3. Molecular orbital calculations of hydrogen storage in BN and C clusters

$\text{B}_{24}\text{N}_{24}$, $\text{B}_{36}\text{N}_{36}$, $\text{B}_{60}\text{N}_{60}$ and C_{60} were selected for cluster calculations. To investigate the optimized structures, semi-empirical molecular orbital calculations (parameterized model revision 5, PM5) were performed by using MOPAC. Eigenvector following (EF) method was used for geometry optimization, and charge is 0. The default self-consistent method was restricted Hartree–Fock. Multi-electron configuration interaction (MECI) was used in order to prevent repulsion between electrons becoming excessive. Chemisorption calculations of hydrogen atoms were performed for $\text{B}_{24}\text{N}_{24}$, $\text{B}_{36}\text{N}_{36}$ and C_{60} by PM5 calculations [11,12].

Figure 4 is a structural model of hydrogen atoms chemisorbed on boron and nitrogen for BN clusters and carbon clusters. Atoms bonded with hydrogen are moved outside from the clusters. Energies for hydrogen chemisorption on each position are summarized as Table 3. Hydrogen bonding with nitrogen is more stable than that with boron, and hydrogen bonding with carbon is more stable than C_{60} . This result indicates the chemical modification of carbon fullerenes. When two hydrogen atoms were chemisorbed on carbon clusters, energies of carbon clusters increased.

In the calculation, chemisorption of hydrogen was performed on outside of cage, and on boron, nitrogen and carbon of tetragonal and hexagonal rings. The $\text{B}_{36}\text{N}_{36}$ cluster has tetragonal and hexagonal BN rings, and there are four kinds of boron and nitrogen positions for the hydrogen chemisorption, as shown in Figure 5. For the stability calculations of H_2 molecules in these clusters, 30 H_2 molecules were also introduced in $\text{B}_{24}\text{N}_{24}$, $\text{B}_{36}\text{N}_{36}$, $\text{B}_{60}\text{N}_{60}$ and C_{60} . Figure 5 is a structural model of hydrogen atoms chemisorbed on boron and nitrogen for $\text{B}_{36}\text{N}_{36}$. Energies for hydrogen chemisorption on each position are summarized as Table 2. Hydrogen bonding with nitrogen is more stable than that with boron because nitrogen atoms are more electrophilic compared to boron atoms. In addition, hydrogen bonding on tetragonal ring is more stable than that of hexagonal ring. Chemisorption of hydrogen with C_{60} reduced the energy. When two hydrogen atoms were chemisorbed on carbon clusters, energies of carbon clusters increased.

Figure 4. Structural models of H atoms chemisorbed on (a) C_{60} and (b) $B_{24}N_{24}$.

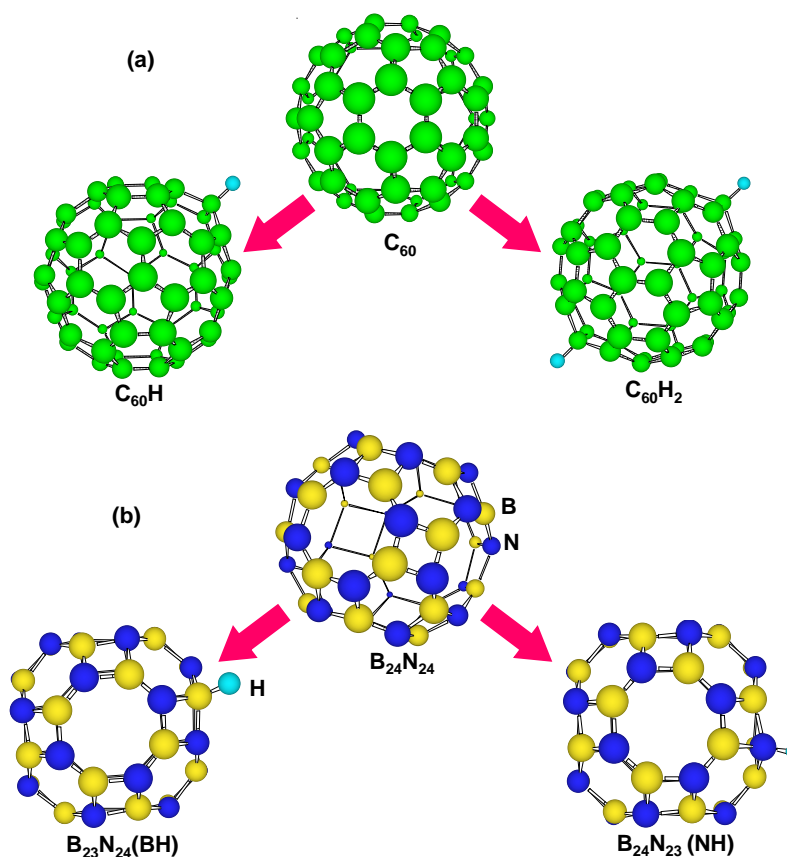


Figure 5. Structure models for hydrogen chemisorption on $B_{36}N_{36}$. (a) Structural model of $B_{36}N_{36}$. (b), (c) Structural models of hydrogen chemisorption on B and N positions of tetragonal BN ring, respectively. (d), (e) Structural models of hydrogen chemisorbed on B and N positions of hexagonal BN ring, respectively.

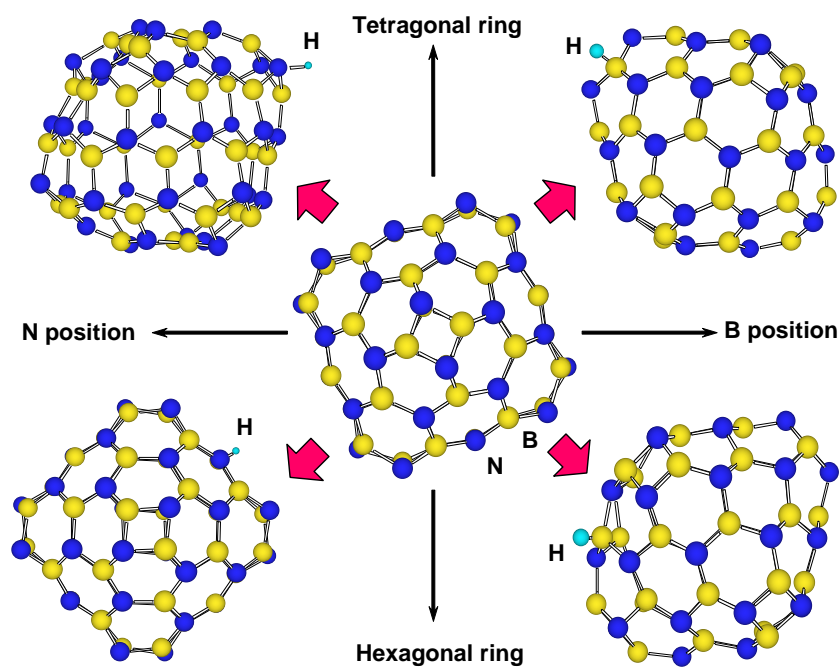
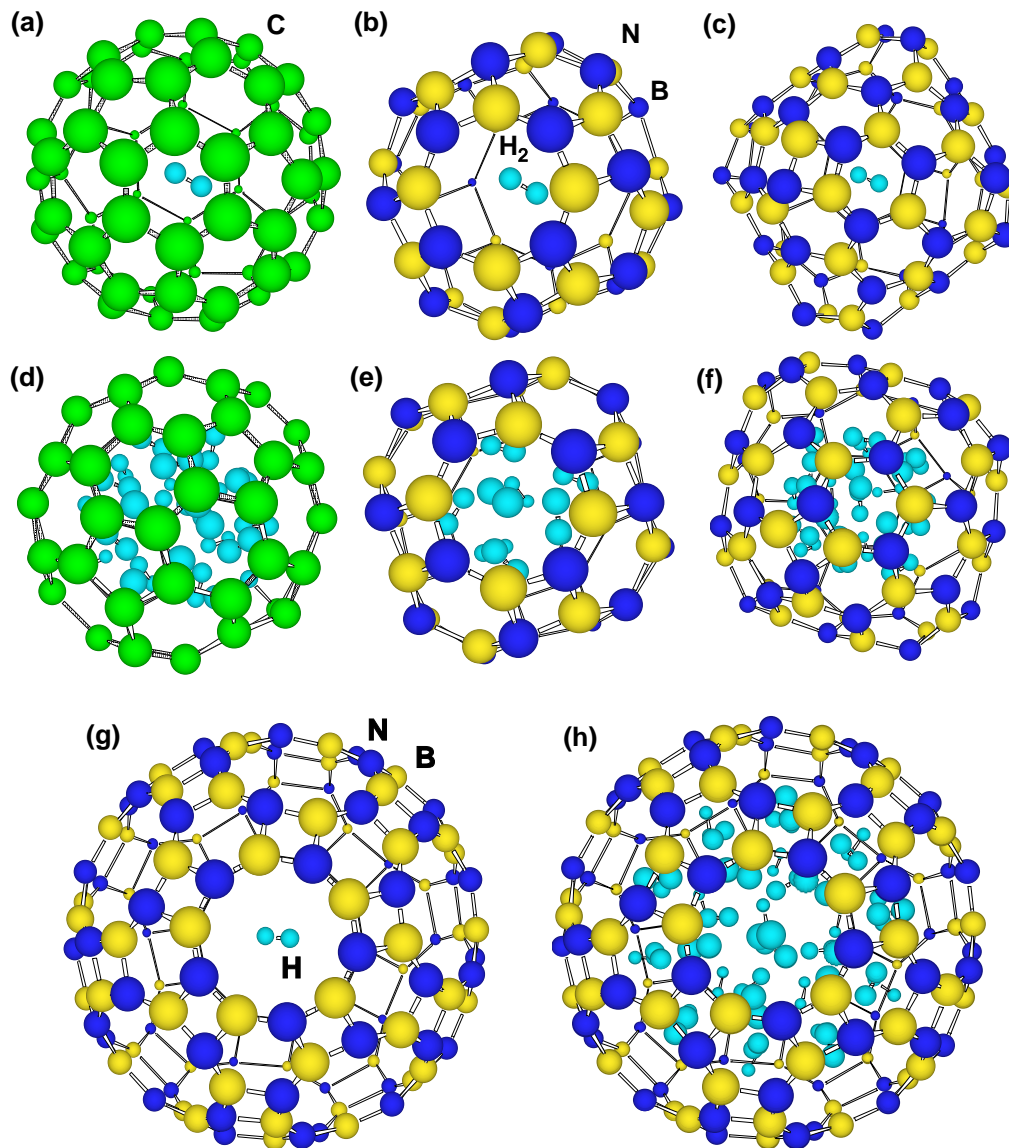


Figure 6. Optimized structural models of H₂ molecules in the clusters. A H₂ molecule in the center of (a) C₆₀, (b) B₂₄N₂₄, (c) B₃₆N₃₆, (d) 22 H₂ molecules inside C₆₀ and 8 atoms chemisorbed, (e) 9 H₂ molecules in B₂₄N₂₄, and (f) 20 molecules in B₃₆N₃₆. (g) 1 and (h) 38 H₂ molecules in B₆₀N₆₀.



To investigate stability of H₂ molecules in clusters, energies were calculated for H₂ molecules introduced in the center of clusters. The structural models are shown in Figure 6. Energies of C₆₀, B₂₄N₂₄, B₃₆N₃₆ and B₆₀N₆₀ were calculated to be 0.58, 20.71, 20.93 and 20.82 eV/mol atom. This result indicates that B₂₄N₂₄, B₃₆N₃₆ and B₆₀N₆₀ with H₂ molecules are more stable than C₆₀ with H₂ molecule, and that B₃₆N₃₆ is the most stable in BN clusters.

Hydrogen storage (wt%) of B₆₀N₆₀ cluster was calculated, and structural models are shown in Figure 7. Other C₆₀, B₂₄N₂₄ and B₃₆N₃₆ were calculated, as summarized in Table 3. From Table 3, C and BN cluster showed possibility of hydrogen storage of ~6.5 and ~4.9 wt%, respectively.

Table 2. Chemisorption energy of hydrogen atoms on C₆₀ and B₂₄N₂₄.

Cluster	Number of hydrogen atoms	Additional position of hydrogen	Heat of formation (eV)		ΔE^* (eV)
			Before addition	After addition	
C ₆₀	1	C	35.21	35.03	-0.18
	2	C	35.21	35.81	0.6
B ₂₄ N ₂₄	1	B	-36.12	-34.66	1.46
	1	N	-36.12	-35.67	0.45
	1	B of tetragonal ring	-69.33	-67.83	1.50
B ₃₆ N ₃₆	1	N of tetragonal ring	-69.33	-69.16	0.17
	1	B of tetragonal ring	-69.33	-67.51	1.83
	1	N of tetragonal ring	-69.33	-68.83	0.51

* $\Delta E = (\text{Heat of formation after hydrogen addition}) - (\text{Heat of formation before hydrogen addition})$

Table 3. Energy of clusters with hydrogen.

Cluster	Introduced H ₂	Heat of formation (eV)	H atoms chemisorbed inside cluster	Hydrogen storage (wt. %)	Heat of formation per added H atom (eV/H atom)
C ₆₀	0	35.21	0		
	22	143.01	0		
	25	164.87	4	5.8–6.5	4.9–5.2
	26	169.63	8*		
B ₂₄ N ₂₄	0	-36.12	0		
	9	-9.44	0	2.9	3.0
B ₃₆ N ₃₆	0	-69.33	0		
	20	-6.66	0	4.3	3.1
B ₆₀ N ₆₀	0	-100.28	0		
	38	-61.74	0	4.9	1.0

*A C-C bond was broken.

Although hydrogen storage (wt%) of C₆₀ is better than those of BN clusters, energy increase by hydrogen addition is higher for C₆₀ (4.6–5.2 eV/H atom) compared to BN clusters (1.0–3.1 eV/H atom), which would be due to C–H interaction. This indicates that needed energy for hydrogen storage in BN clusters is lower compared to the C₆₀. From Table 3, stability of H₂ molecules in B₂₄N₂₄ and B₃₆N₃₆ seems to be higher than that of C₆₀. Hydrogen atoms were calculated to be chemisorbed inside C₆₀, as shown in Table 1. This indicates that inside of C₆₀ also has good reactivity as well as outside of the cage. Chemisorption inside the C₆₀ clusters may indicate that hydrogen capacity may gradually reduce under the adsorption–desorption cycles. On the other hand, BN clusters have no chemisorption inside the clusters, which indicates that the BN clusters would be a better candidate for stable adsorption–desorption cycles. C₆₀ cluster shows the minimum energies in spite of the positive values. It is believed that p-electrons outside and inside of the cage would increase the energy. However, s-electrons in the

5- and 6-membered carbon rings would stabilize the cage structure. Hydrogen addition to the C_{60} decreased the energy, which agrees with the above description.

Carbon nanotubes are oxidized at 600 °C in air. On the other hand, BN are stable up to 1000 °C in air, which indicates BN fullerenes have higher thermal and chemical stability than those of carbon fullerenes. BN fullerenes with good thermal and chemical stability can store H_2 molecules with less energy, and they have the same chemisorption energy and higher stability, compared to carbon clusters. BN fullerene materials would be better candidates for H_2 storage materials.

4. Effects of endohedral element in $B_{24}N_{24}$ clusters on hydrogenation

$M@B_{24}N_{24}$ ($M@$: element encaged in $B_{24}N_{24}$) was selected for cluster calculations. To investigate the optimized structures, semi-empirical molecular orbital calculations were performed by using PM5 in MOPAC. The EF method was used for geometry optimization. The default self-consistent method was restricted Hartree-Fock. The MECI was used in order to prevent repulsion between electrons becoming excessive. Chemisorption calculations of hydrogen atoms were performed for $M@B_{24}N_{24}$ by PM5 calculations. In the calculation, chemisorption of hydrogen was performed on boron and nitrogen positions outside the cage [13]. Energy levels and densities of states (DOS) for $B_{24}N_{24}$ and $Li@B_{24}N_{24}$ were also calculated by the first principles calculation with discrete variational (DV)-X α method.

Figure 7. Structural models for (a) $B_{24}N_{24}$, (b) endohedral $M@B_{24}N_{24}$, (c) hydrogenated $M@B_{24}N_{24}-H$ and (d) $M@B_{24}N_{24}$ which chemisorbed 24 hydrogen atoms.

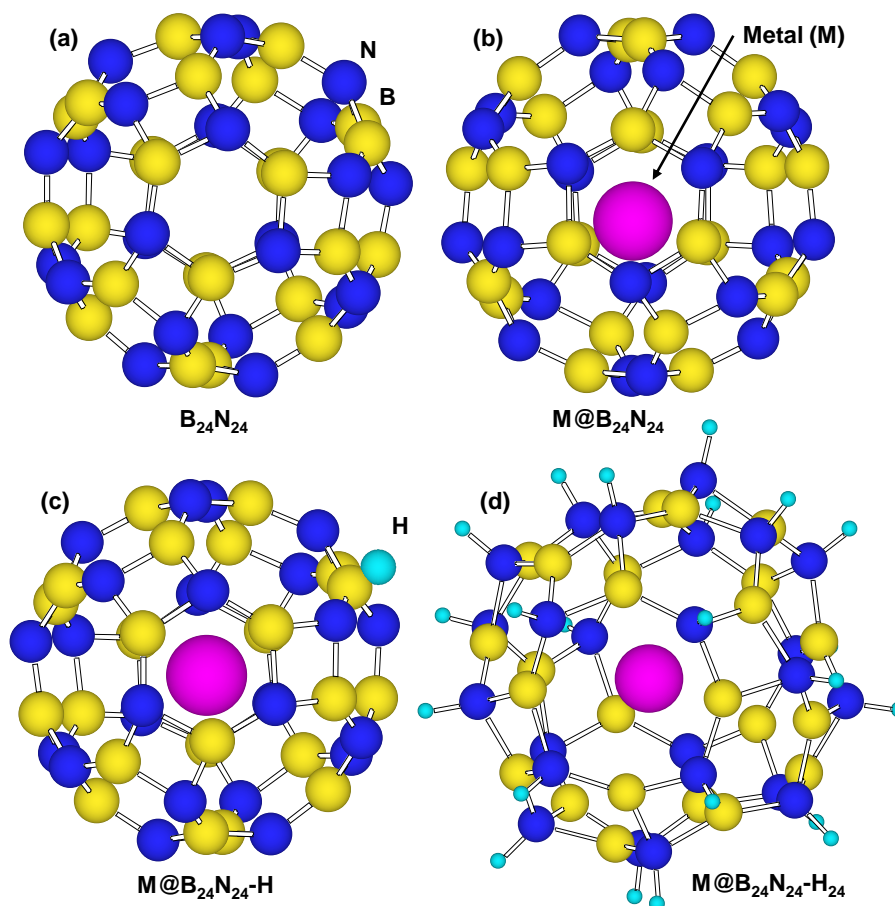


Figure 8. Heats of formation of hydrogenation for $M@B_{24}N_{24}$ clusters by endohedral elements.

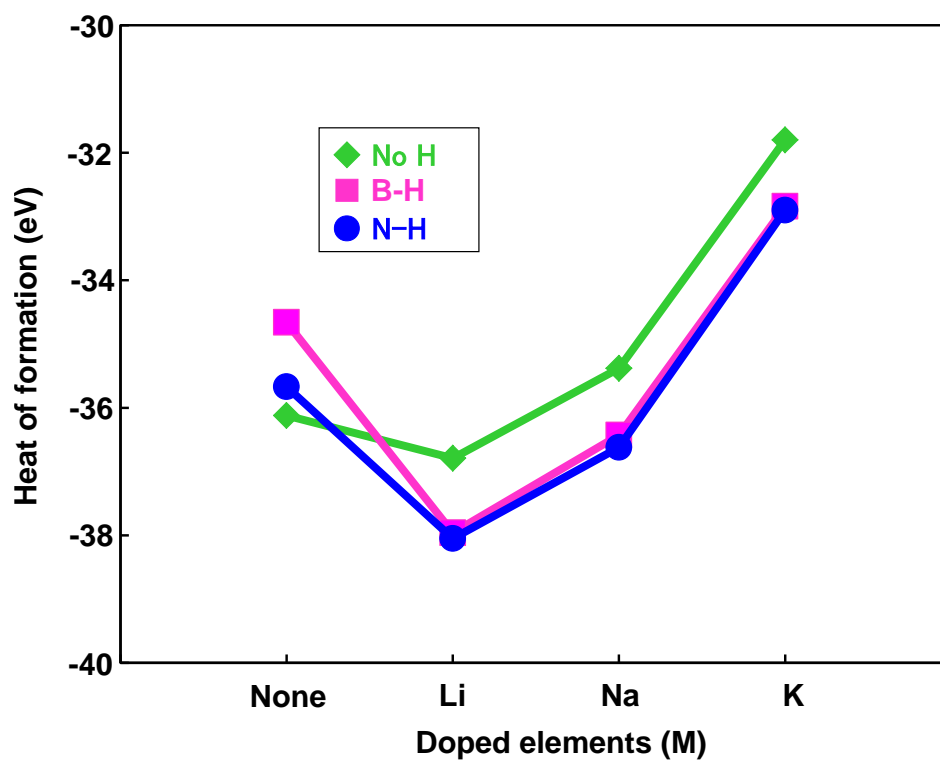


Table 4. Chemisorption energies of a hydrogen atom on $M@B_{24}N_{24}$.

Cluster	Hydrogenation position	Heat of formation (eV)	ΔE^* (eV)
$B_{24}N_{24}$	Un-hydrogenated	-36.12	0
	B	-34.66	1.46
	N	-35.67	0.45
$Li@B_{24}N_{24}$	Un-hydrogenated	-36.79	0
	B	-37.96	-1.17
	N	-38.05	-1.26
$Na@B_{24}N_{24}$	Un-hydrogenated	-35.38	0
	B	-36.43	-1.05
	N	-36.62	-1.24
$K@B_{24}N_{24}$	Un-hydrogenated	-31.80	0
	B	-32.84	-1.04
	N	-32.90	-1.10

* $\Delta E = (\text{heat of formation after hydrogen addition}) - (\text{heat of formation before hydrogen addition})$.

Table 5. Bond length of B–H and N–H on $M@B_{24}N_{24}$.

Cluster	B–H (Å)	N–H (Å)
$B_{24}N_{24}$	1.229	1.010
$Li@B_{24}N_{24}$	0.695	0.616
$Na@B_{24}N_{24}$	1.203	1.005
$K@B_{24}N_{24}$	1.204	1.006

Table 6. Hydrogen storage capacity of chemisorption on nitrogen position of $M@B_{24}N_{24}$.

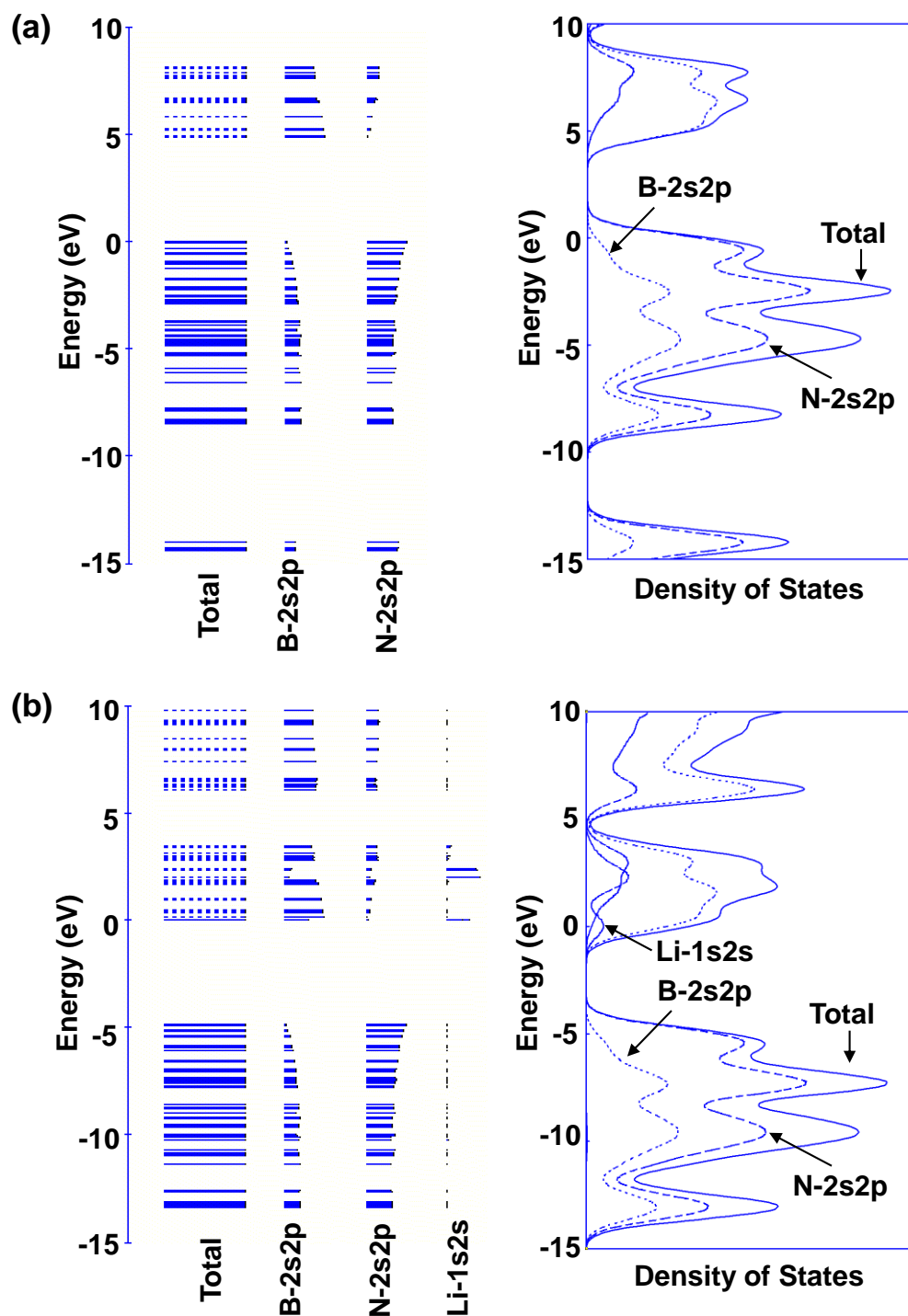
Cluster	Hydrogen storage (wt%)
$Li@B_{24}N_{24}H_{24}$	3.86
$Na@B_{24}N_{24}H_{24}$	3.76
$K@B_{24}N_{24}H_{24}$	3.67

Figure 7 is a structural model of hydrogen atoms chemisorbed on nitrogen position for $M@B_{24}N_{24}$. Energies for hydrogen chemisorption on boron and nitrogen positions are summarized as Table 4.

Heats of formation (eV) of $M@B_{24}N_{24}$ by hydrogenation are indicated in Fig. 8. In Table 4 and Fig. 8, “None” means that metal catalyst was not encaged in $B_{24}N_{24}$, and “BH” and “NH” means that hydrogen atom was chemisorbed on boron and nitrogen, respectively. Figure 8 shows that hydrogen bonding with nitrogen is more stable than that with boron because nitrogen atoms are more electrophilic compared to boron atoms. Figure 8 also indicates that energies of chemisorption on $M@B_{24}N_{24}$ are much lower than that of $B_{24}N_{24}$. From this result, Li atom works as a good endohedral element for hydrogen chemisorption. Metal catalysts in the present work have been reported to generate hydrides such as LiH because of strong interaction between hydrogen and metal atoms. In the present work, it is clarified that Li doping and nitrogen positions are suitable for hydrogenation for the $B_{24}N_{24}$ clusters.

Bond lengths of B–H and N–H for $M@B_{24}N_{24}$ are summarized in Table 5. B–H and N–H distance decreased by doping element in the BN cluster. Bond lengths of N–H are shorter than that of B–H for these BN clusters, and the bond length of N–H for $Li@B_{24}N_{24}$ is the shortest. The endohedral atoms appear to decrease the repulsion energy between the electrons of the hydrogen atom and the p-electrons of $B_{24}N_{24}$. Figure 7(d) is a structural model of $M@B_{24}N_{24}H_{24}$, which indicates hydrogenation on all nitrogen positions for $M@B_{24}N_{24}$, and the hydrogen storage capacity is summarized in Table 6. Li is also a good element for hydrogen storage capacity because Li is the lightest element of these. Energy levels and density of states for $B_{24}N_{24}$ and $Li@B_{24}N_{24}$ are shown in Figure 9. Fermi levels in energy level diagrams and DOS diagrams correspond to 0 eV. $B_{24}N_{24}$ and $Li@B_{24}N_{24}$ show energy gaps of 4.8873 and 0.0247 eV between the highest occupied molecular orbital (HOMO) and the lowest unoccupied molecular orbital (LUMO), respectively. This means that electron of Li element transferred to the $B_{24}N_{24}$ cage, and electronic state of BN cluster would change from semiconductor to metallic property by Li doping in BN clusters.

Figure 9. Energy levels diagrams and density of states of (a) $B_{24}N_{24}$ and (b) $Li@B_{24}N_{24}$.



Although it was reported that BN nanotubes were produced by lithium vapor, synthesis of $Li@BN$ has not been reported yet. BN fullerenes have high thermal and chemical stability, and $M@BN$ fullerenes have lower energy of chemisorption compared to the present work. Since the BN clusters were reported to be doped with metal elements, $M@BN$ clusters would be produced. BN fullerene materials with endohedral element such as Li would be better candidates for H_2 storage materials.

5. Molecular dynamics calculations of hydrogen storage in C₆₀ clusters

Molecular dynamics calculations were carried out to confirm the stability of H₂ molecules into C₆₀ at 298 K and 0.1 MPa [14]. NTP ensembles were used in the calculation as follows: number of atoms (N), temperature (T) and pressure (P) are constant. Conditions of H₂ gas storage were also calculated. NPH ensembles were used in the calculation as follows: number of atoms (N), pressure (P) and enthalpy (H) are constant. These molecular dynamics were calculated by organic potential.

C₆₀ included a H₂ molecule kept in stable state at T=298 K and P=0.1 MPa. This unit cell is shown in Figure 10. This model was calculated with N=62 atoms, T=298 K and P=0.1 MPa. Although the H₂ molecule vibrated in the C₆₀ cage, it was not discharged from the cage. Some H₂ molecules were stored in the C₆₀ cage when the pressure was 5 MPa. This unit cell is shown in Figure 11, which is composed of 32C₆₀ (fcc) with 288 H₂ molecules (fcc). This model was calculated with N=2496 atoms and P=5 MPa. H₂ molecules pass through the hexagonal rings of the C₆₀ cage at 0.5 ps.

After introducing H₂ molecules into the C₆₀ cage at 2.5 ps, they are stored and stable in C₆₀. Figure 12 shows a schematic model of a single H₂ molecule stored in a hexagonal ring of C₆₀. These results indicate that fullerene-like materials can store H₂ gas in cage at T=298 K and P=0.1 MPa, and some H₂ molecules were stored in the C₆₀ cage when the pressure was greater than 5 MPa. It is known that H₂ molecules are adsorbed on the walls of single-walled carbon nanotubes over 7 MPa as an experimental result [15]. Since a C₆₀ cluster has a large curvature and H₂ molecules are very small compared to C₆₀, it is considered that adsorption and storage of H₂ gas occur at the same time.

Figure 10. Molecular dynamics calculation to confirm stability of H₂ molecule into C₆₀ at 298 K and 10⁵ Pa. NTP ensembles and organic potential were used in the calculation.

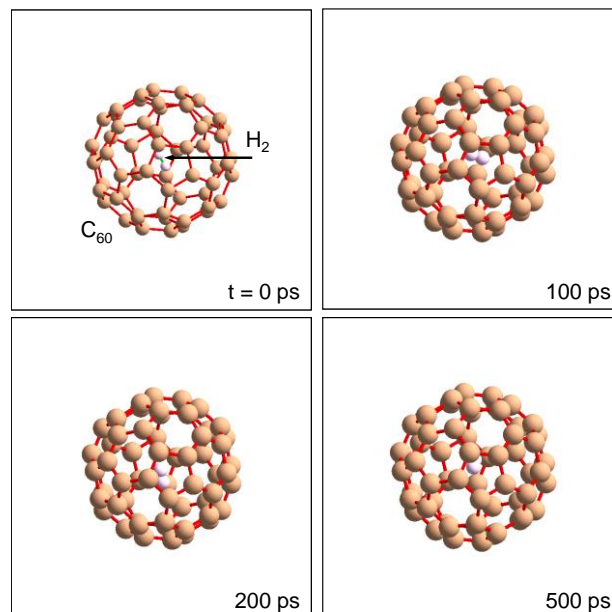


Figure 11. Molecular dynamics calculation to find condition of H_2 gas storage. Unit cell is composed from $32C_{60}$ (fcc) with 288 H_2 molecules (fcc). NPH ensembles and organicpotential were used in the calculation.

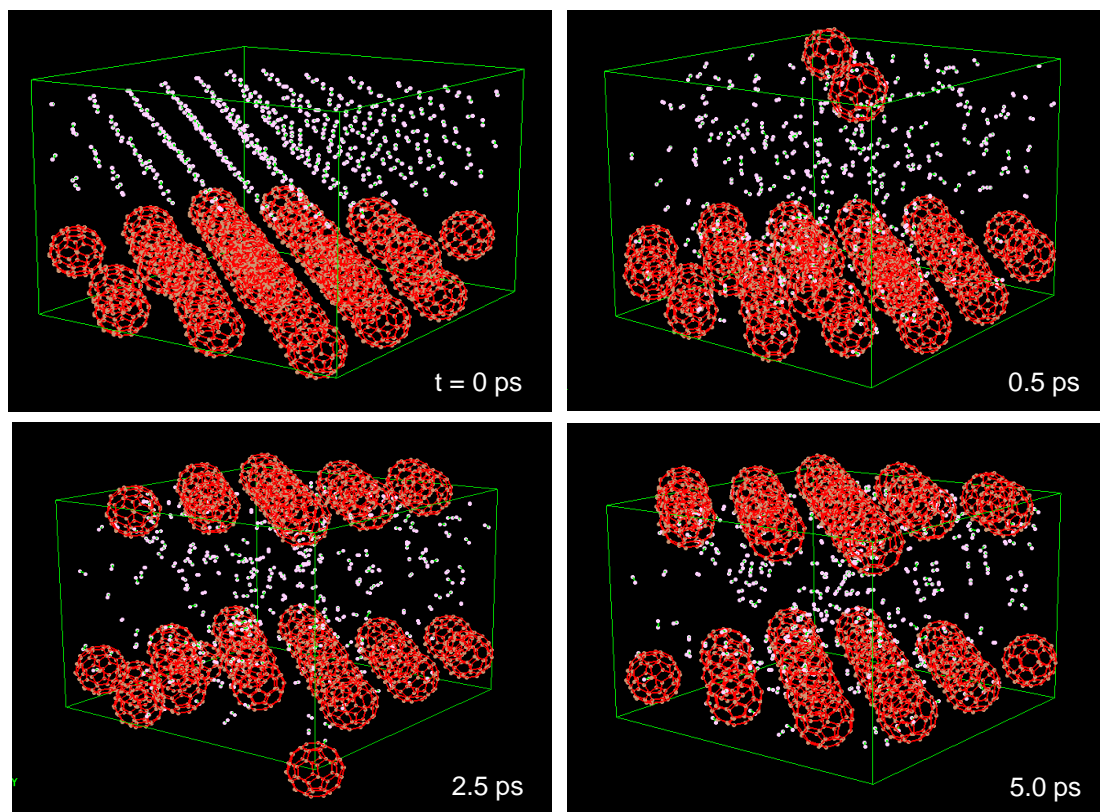
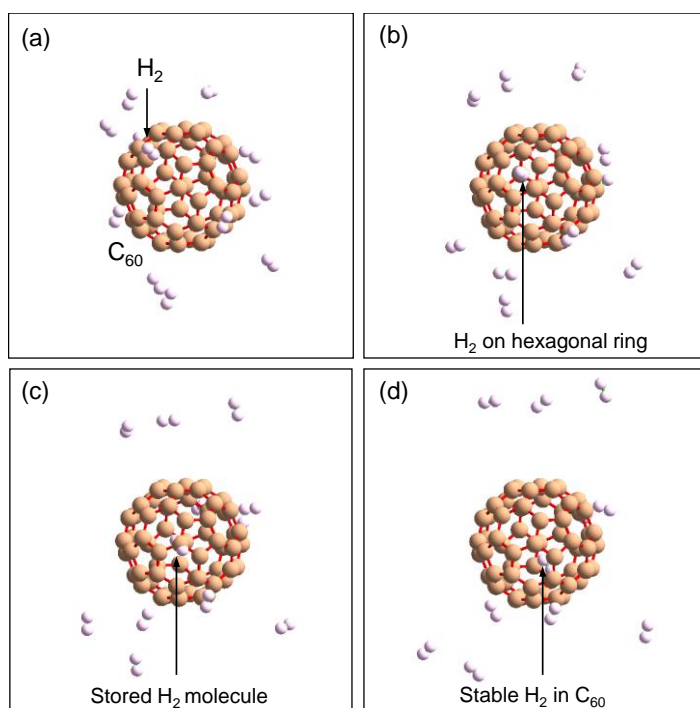


Figure 12. Schematic model of H_2 molecule stored in hexagonal ring in the order of (a), (b), (c), and (d).



6. Conclusions

HREM observation showed the formation of BN nanotubes, nanocapsules and nanocages, which were synthesized from mixtures of LaB₆, Pd, and boron powder by using an arc melting method. Although samples produced with Pd include only BN nanocapsule structures, samples produced with LaB₆ present BN nanocapsule, nanotube and nanocage structures. After separation of BN nanomaterials using ethanol, hydrogen storage was measured by TG/DTA, and the BN nanomaterials produced from LaB₆ and Pd/boron powder showed possibility of hydrogen storage of ~3 wt%. Energies for BN and C clusters with hydrogen were investigated by molecular orbital calculations. Stabilities of these clusters were estimated from the energies, and possibility of H₂ storage ability was predicted by these results. B₂₄N₂₄, B₃₆N₃₆, B₆₀N₆₀ and C₆₀ clusters were selected as the tip structure of the nanotubes. Chemisorption calculation of hydrogen for BN clusters showed that hydrogen bonding with nitrogen atoms was more stable than that with boron atoms, and that hydrogen bonding with tetragonal ring is more stable than that with hexagonal ring. Energy increase by hydrogen addition to C₆₀ is higher compared to BN clusters because of C–H interaction, which indicates that the BN clusters have higher stability with hydrogen atoms. BN cluster and C cluster showed possibility of H₂ storage of ~4.9 wt% and ~6.5 wt%, respectively. H₂ storage of C cluster is better than those of BN clusters. However, stability of H₂ molecules in BN clusters might be higher than that of C clusters. Energies of hydrogenation for B₂₄N₂₄ were also investigated by molecular orbital calculations. Chemisorption calculation of hydrogen in the B₂₄N₂₄ clusters showed that hydrogen bonding with nitrogen atoms was more stable than that with boron atoms. Chemisorption calculations also indicate that endohedral elements decreased energies of hydrogenation and Li atom is suitable element for hydrogen chemisorption. Molecular dynamics calculations showed that a single H₂ molecule remains in a stable state in a C₆₀ cage at T=298 K and P=0.1 MPa. It is confirmed that pressure of over 5 MPa is required to store H₂ molecules in a C₆₀ cage. As a result of SPE calculations, H₂ molecules enter from hexagonal rings of fullerene-like materials. The energy required of H₂ discharge from fullerene-like materials is similar to that of H₂ storage. The present study indicates that BN fullerene materials could be a one of the possible candidates as hydrogen gas storage materials.

Acknowledgments

The author would like to acknowledge N. Koi, M. Kuno, I. Narita, M. Inoue and K. Suganuma for excellent collaborative works and useful discussion.

References and Notes

1. Schlapbach, L.; Züttel, A. Hydrogen-storage materials for mobile applications. *Nature* **2001**, 414, 353-358.
2. Dillon, A.C.; Jones, K.M.; Bekkedahl, T.A.; Kiang, H.; Bethune, D.S.; Heben, M.J. Storage of hydrogen in single-walled carbon nanotubes. *Nature* **1997**, 386, 377-379.
3. Chen, P.; Wu, X.; Lin, J.; Tan, K.L. High H₂ uptake by alkali-doped carbon nanotubes under ambient pressure and moderate temperatures. *Science* **1999**, 285, 91-93.

4. Dujardin, E.; Ebbesen, T.W.; Hiura, H.; Tanigaki, K. Capillarity and wetting of carbon nanotubes. *Science* **1994**, 265, 1850-1852.
5. Liu, C.; Fan, Y.Y.; Liu, M.; Cong, H.T.; Cheng, H.M.; Dresselhaus, M.S. Hydrogen storage in single-walled carbon nanotubes at room temperature. *Science* **1999**, 286, 1127-1129.
6. Nützenadel, C.; Züttel, A.; Chartouni, D.; Schlapbach, L. Electrochemical storage of hydrogen in nanotube materials articles. *Electrochem. Solid-State Lett.* **1999**, 2, 30-32.
7. Wu, X.B.; Chen, P.; Lin, J.; Tan, K.L. Hydrogen uptake by carbon nanotubes. *Int. J. Hydrogen Energy* **2000**, 25, 261-265.
8. Oku, T.; Narita, I.; Koi, N.; Nishiwaki, A.; Suganuma, K.; Inoue, M.; Hiraga, K.; Matsuda, T.; Hirabayashi, M.; Tokoro, H.; Fujii, S.; Gonda, M.; Nishijima, M.; Hirai, T. Belosludov RV and Kawazoe Y. Boron nitride nanocage clusters, nanotubes, nanohorns, nanoparticles, and nanocapsules. In: Yap YK ed. *B-C-N nanotubes and related nanostructures*. Springer, **2009**, 149-194.
9. Oku, T. Direct structure analysis of advanced nanomaterials by high-resolution electron microscopy. *Nanotechnol. Rev.* **2012**, 1, 389-425.
10. Oku, T.; Kuno, M.; Narita, I. Hydrogen storage in boron nitride nanomaterials studied by TG/DTA and cluster calculation. *J. Phys. Chem. Solids* **2004**, 65, 549-552.
11. Oku, T.; Narita, I. Calculation of H₂ gas storage for boron nitride and carbon nanotubes studied from the cluster calculation. *Physica B* **2002**, 323, 216-218.
12. Koi, N.; Oku, T. Hydrogen storage in boron nitride and carbon clusters studied by molecular orbital calculations. *Solid State Commun.* **2004**, 131, 121-124.
13. Koi, N.; Oku, T.; Suganuma, K. Effects of endohedral element in B₂₄N₂₄ clusters on hydrogenation studied by molecular orbital calculations. *Physica E* **2005**, 29, 541-545.
14. Oku, T.; Narita, I.; Nishiwaki, A.; Koi, N.; Suganuma, K.; Hatakeyama, R.; Hirata, T.; Tokoro, H.; Fujii, S. Formation, atomic structures and properties of carbon nanocage materials. *Topics Appl. Phys.* **2006**, 100, 187-216.
15. Ye, Y.; Ahn, C.C.; Witham, C.; Fultz, B.; Liu, J.; Rinzler, A.G.; Colbert, D.; Smith, K.A. and Smalley, R.E. Hydrogen adsorption and cohesive energy of single-walled carbon nanotubes. *Appl. Phys. Lett.* **1999**, 74, 2307-2309.